A High Payload Aerial Platform for Infrastructure Repair and Manufacturing

Lachlan Orr[1,2], Brett Stephens[1,2], Basaran Bahadir Kocer[1] and Mirko Kovac[1,2]

***Abstract*—The use of aerial robots in construction is an area of general interest in the robotics community. Autonomous aerial systems have the potential to improve safety, efficiency and sustainability of industrial construction and repair processes. Several solutions have been deployed in this domain focusing on problems in aerial manipulation and control using existing aerial platforms which are not specialised for the specific challenges in operating on a construction site. This paper presents a new compact, high thrust aerial platform that can act as a modular, application agnostic base for demonstrating a wide variety of capabilities. The platform has been built and tested flying both with manual controls and autonomously in a motion tracking arena while carrying a payload of up to $7.3\,\mathrm{kg}$ with a maximum flight time between 10–$34\,\mathrm{mins}$ (payload dependent). In the future, this platform will be combined with vision based tracking sensors, manipulators and other hardware to operate in and interact with an outdoor environment. Future applications may include manipulation of heavy objects, deposition of material and navigating confined spaces.**

I. Introduction

Robotic and autonomous systems have opened up new and exciting opportunities in the field of architecture and construction [1]. These systems promise to improve safety, efficiency and sustainability on construction sites [2]. Construction work is a high-risk occupation: for instance in the United Kingdom, there were 40 fatal injuries in the 2019/2020 period [3] and 20 of these were falls from height. Aerial robotic systems are proposed as a viable solution to remove the need for human workers to be exposed to this level of risk, while also greatly improving speed and reducing cost by removing the need to erect scaffolding or other temporary supporting structures. These systems will need to operate in both open and enclosed spaces and will require on-board sensing and decision making capability to complete various construction and repair tasks.

There is a considerable body of literature on aerial robots performing various tasks during flight through free space, however, interaction with a solid environment presents new challenges. This has been explored in a number of different contexts such as inspection [4], material transportation [5], sensor installation [6], material deposition [7], and aerial manipulation [8]. The complexity of the applications may require the systems to be structurally morphic [9], or have additional degrees of freedom in flight [10]. Interaction with surfaces may require compliant [11] or soft [12] components. Furthermore, the associated vision, navigation, and control modules need to handle emergent challenges where reactive navigation [13] and online adaptation with correction [14] play a vital role. When these modules are leveraged on board a high payload aerial robot, a significant improvement in the efficiency, cost and safety of infrastructure operations at height is anticipated.

Aerial transportation, physical interaction and contact flight all require additional complex hardware which increases the payload requirements for the system. The additional level of dexterity and degrees of freedom granted by an aerial manipulator, for instance, must not be outweighed by the performance penalty due to the increased weight of the system. Aerial repair and infrastructure manufacturing will also require the transportation of heavy tools and materials. Large platforms interacting with surfaces will generate higher wrench torques from the end-effector in contact making accurate and energy efficient positioning more difficult. Their size will also increase disturbance forces from wind and wall and ground effects. To the best of the authors' knowledge, there is still no well designed large aerial platform with a payload of $5\,\mathrm{kg}$+ that is capable of operating in confined spaces for construction tasks.

This paper presents a custom-built, application agnostic, high payload platform to facilitate work in aerial infrastructure repair and manufacturing. Existing work and the challenges of operating an aerial vehicle in a construction environment are discussed. A custom system is designed and built and early experimental evaluation of the flight performance is presented. Future plans for the platform are also discussed, including additional sensing and computation requirements for outdoor operation and the potential of increasing the payload further with upgraded components.

II. Challenges

Aerial repair and infrastructure manufacturing require precise spatial localisation in a changing outdoor environment. Flying robots are subjected to various disturbances (such as wind gusts) and current approaches to compensate for this leverage closed-loop control architectures for stability, tracking and adaptation. However, aerial platforms are still unlikely to be able to compete with heavy ground based systems in pure end-effector precision. One solution to this is to implement loop closure at the vision level and compensate for errors based on visual measurements of the task in progress [15].

[1]The authors are with the Aerial Robotics Laboratory, Imperial College London, London SW7 2AZ, UK. [2]The authors are with the Materials and Technology Center of Robotics at the Swiss Federal Laboratories for Materials Science and Technology, Switzerland.

TABLE I: Levels of autonomy in aerial construction demonstrations.

Level of autonomy	Description	Examples
Low autonomy	Low level pitch/yaw/roll commands controlled by a human operator.	[17]
Sensory-motor autonomy	Follow pre-determined trajectories.	[18], [19], [20]
Reactive autonomy	Account for environmental disturbances during the construction process and make simple corrections, interact with fixed surfaces.	[4], [6], [7]
Cognitive autonomy	Map a structure (either when in need of repair or during the construction) during a task to make trajectory corrections and perform structural assessment. Coordinate with other agents on a construction site to complete a task.	Yet to be achieved

Table I summarises the level of autonomy in existing aerial construction systems based on a framework adapted from Floreano et al. (2015) [16]. This ranking is intended to broadly cover a wide spectrum of autonomous behaviour from pure manual control through to high level decision making and visual closed-loop manufacturing.

A platform capable of facilitating closed-loop manufacturing and repair tasks (with continuous structural mapping and assessment) will need to be able to carry construction materials, a manipulator/associated deposition hardware and onboard SLAM sensors. These components all add considerable weight to the system. It must also be capable of navigating a construction site and interacting with the build as it progresses. As the system becomes larger, it will become more difficult to navigate through and around obstacles. Also, an architect designing an aerially manufactured structure will have reduced freedom if consideration must be made for access and egress of aerial vehicles from the construction site. Therefore it is desirable to produce a platform with high thrust that is also as compact as possible. The key requirements for the platform are summarised below:

1) Sufficiently high payload to carry standard construction materials (bricks/cement/glues and sprays in standard canisters), manipulators and sensors.
2) Support an aerial manipulator and have sufficient thrust to account for movements in centre of mass and end-effector disturbances.
3) Modular design to allow in-situ repairs on the construction site. As many parts as possible to be manufacturable on-site using rapid prototyping processes.
4) Physical compatibility with construction environment (must fit through doorways/windows), be small enough relative to structure for cooperative swarms to be feasible.

III. Platform Design

It is assumed that the flight speeds during construction activities will always be low (less than $1\,\mathrm{ms}^{-1}$) and that the altitude above ground level will seldom exceed $100\,\mathrm{m}$. Therefore, the design and sizing of the platform has revolved around optimising the hover endurance for a given payload.

TABLE II: Major pre-fabricated components list.

Compute module	NVIDIA® Jetson™ TX2
Flight Controller	Holybro Pixhawk 4
Tracking camera	Intel® Realsense™ T265
Depth Camera	Intel® Realsense™ D435i
Batteries	3× Turnigy 6600 mAh 6S 12C LiPo Pack
Motors	6× T-motor MN501-S KV240
ESC	6× T-motor AIR 40 A 6S
Propellers	6× T-motor 22×6 inch folding

In similar construction based demonstrations [7], a payload of approx. $2.5\,\mathrm{kg}$ with a maximum flight time of $5\,\mathrm{mins}$ was required. The new platform has been designed to double this capability in both performance metrics (i.e. a payload of $5\,\mathrm{kg}$ for $10\,\mathrm{mins}$). In order to facilitate indoor testing, the overall volume of the frame was limited to fit within $1\,\mathrm{m}^3$ (not including rotors). The main components selected to meet this mission profile are listed in Table II.

For the frame, a coaxial tri-rotor arrangement has been selected to address the challenge of maintaining a high thrust and payload capacity while minimising overall size. Figure 1 shows the difference in footprint between a coaxial configuration and a conventional hexarotor. A conventionally arranged platform with the same motor/propeller specifications would be prohibitively large for indoor operation (estimated to be $\approx 2\,\mathrm{m}$ diameter). Furthermore, the distance from the centre of mass of the platform to any hardware projected forwards, clear of the rotors (such as has been demonstrated in aerial manipulation applications [21]), is greatly reduced in a coaxial configuration. This will, in turn, reduce perturbing moments due to the movement of a manipulator or an external wrench due to surface contact.

The main disadvantage of this configuration is the efficiency penalty due to the interaction between the co-axially mounted pairs of rotors. Downwash from the upper rotor reduces the apparent angle of attack of the lower rotor and therefore the thrust generated by the lower rotor is expected to be around $70\,\%$ of the upper. When the rotors are moved closer together (when separation distance $< 0.15\times$rotor diameter), the thrust of the lower rotor can approach 95% of the upper (however this increases the total power requirements of the pair significantly) [22]. The motor spacing on the platform can be modified by adding spacers and a full experimental evaluation of the performance of the coaxial rotor pair mounted on a thrust balance is planned in future. This efficiency loss negatively impacts performance but is thought to be worthwhile in this application due to the significant reduction in platform size. A custom frame was designed and manufactured in-house. This has reduced the overall cost of the system and allows replacement components to be manufactured at short notice in case of damage. Additionally, it provides a high level of flexibility for equipment mounting and future modification. On-site repair is simplified as carbon fibre spares can be CNC or water jet cut in advance and swapped as needed, while plastic components can be 3D printed at the construction site. From previous practical experience, it has been found that propeller guards greatly reduce incidences of propeller

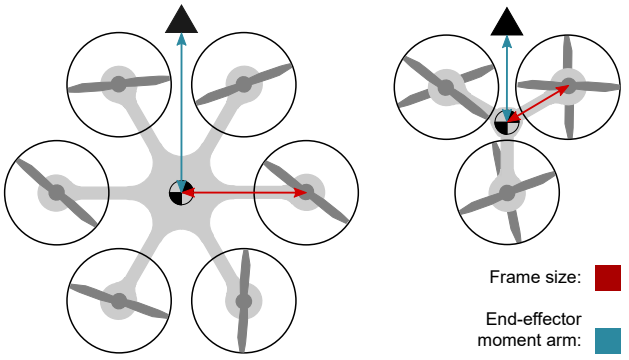

Fig. 1: Frame size comparison between a conventional hexarotor and a coaxial tri-rotor arrangement.

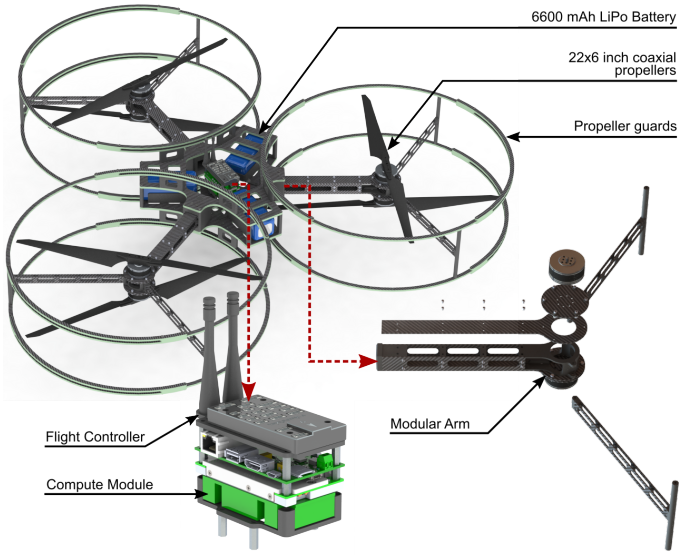

Fig. 2: CAD render of the platform with most major components installed. The central compute + flight controller stack and the arms are easily removable and replaceable to make troubleshooting and repairs on the construction site simpler and faster.

damage (especially in the event of unsteady landings and low-speed contact with solid walls), but are unlikely to improve survivability in the event of a high speed crash or fall from height. The prop guard supports have been designed to buckle preferentially to the rest of the frame in the event of a high-speed impact, but are strong enough to support the full weight of the platform when stood up vertically. This reduces the potential of damage when being handled by an operator for purposes of sensor calibration and transport.

The platform also carries an NVIDIA® Jetson™ TX2 on-board compute module to facilitate autonomous decision making in future projects along with a Pixhawk 4 (PX4) open-source flight controller.

IV. Experimental Evaluation

To-date, the platform has undergone manual flight controller PID tuning and has been flown autonomously in the Imperial College Aerial Robotics Lab's $10 \times 6.2 \times 5.5\,\mathrm{m}$ Vicon motion tracking arena (shown in Figure 3) [23]. The total vehicle

Fig. 3: Flight testing of the platform in the motion tracking arena with a $12.45\,\mathrm{kg}$ take-off mass.

TABLE III: System dimensions and experimentally measured flight performance parameters.

System length	[mm]	1221
Frame size	[mm]	405
Total system mass (no payload)	[kg]	7.3
Max. thrust	[N]	175
Thrust to weight ratio (no payload)	-	2.45
Hover endurance	[mins]	34

life flight time stands at $2\,\mathrm{hours}$. Initial manual flight testing of the vehicle verified that the frame was sufficiently stiff to withstand vibrations from the motors and maneuvering in flight without noticeable deflection. Initial performance parameters measured from this phase of testing are provided in Table III.

Additional manual flight testing was performed with 3 different payload masses (up to an additional $7.3\,\mathrm{kg}$), these masses were achieved by adding additional batteries above and below the 3 battery slots (this can be see in Figure 3). By averaging the throttle level over the duration of the flights, the required throttle to maintain a stable hover was estimated. Power consumption data from the motors was then used to estimate the flight time of a fully charged vehicle. The thrust-to-weight ratio (TWR) was estimated by dividing the thrust at $100\,\%$ throttle by the total mass of the vehicle at each payload level. These values are compared with those provided in the motor/propeller manufacturer data sheet [24] in Figure 4. The thrust measured experimentally was approximately $75\,\%$ of the predicted values. This was expected due to the coaxial rotor interaction discussed in Section III and was accounted for in the platform design and component selection.

Analysis of the flight logs also revealed significant vibrations being transmitted through the frame to the flight controller IMU. Figure 5 shows a peak at $16-18\,\mathrm{Hz}$. Adding mass to the frame appears to damp this frequency along the roll axis.

The platform was finally tested flying with varying payloads while following a circular trajectory in the tracking arena. Figure 6 shows the variation in trajectory tracking errors with payload mass. This evaluation is based on the built-in PID controller in Pixhawk. When precise tracking is required for

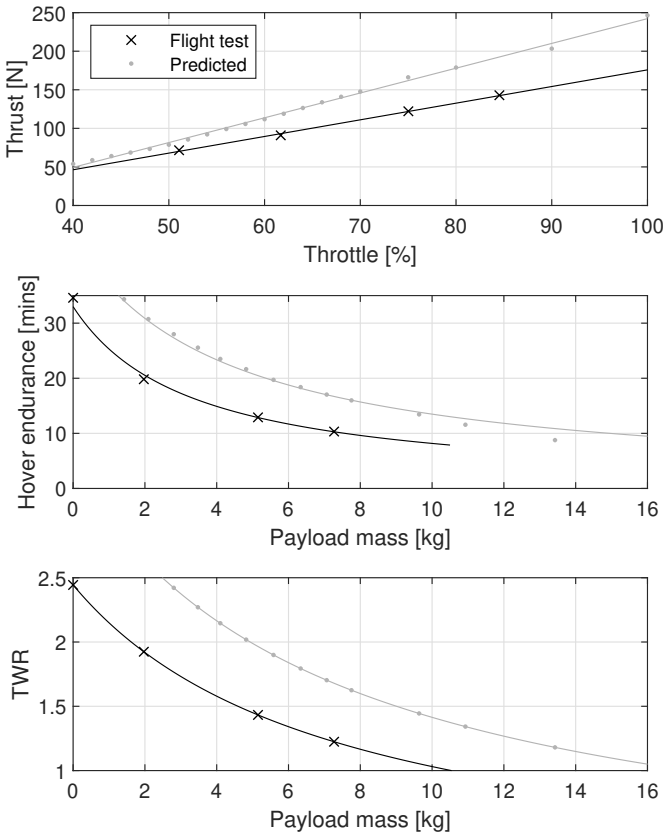

Fig. 4: Plots comparing the measured flight performance compared to the values predicted from the motor/propeller specifications. Efficiency losses due to the coaxial configuration were not accounted for. Flight testing has revealed a 75% performance reduction due to coaxial rotor interactions.

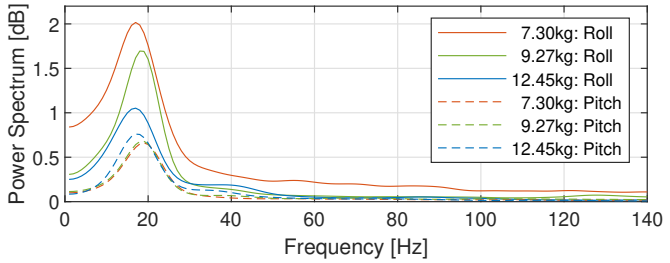

Fig. 5: Power spectrum of angular acceleration in pitch and roll during manual flight testing with various payloads

the construction task, this can be further tuned or accompanied with an error compensation scheme.

V. Discussion

The most concerning characteristic uncovered by the experiments was the high IMU vibration along the pitch and roll axes. High vibration can lead to reduced flight performance and faster component wear [25]. The derivative gains in the PID flight controller also needed to be kept very low as they can become destabilising when applied to a noisy signal. Future work will be undertaken to reduce frame vibration (which will likely improve flight performance and trajectory following accuracy). One possibility that will be investigated is adding compliant vibration isolating mounts for the motors.

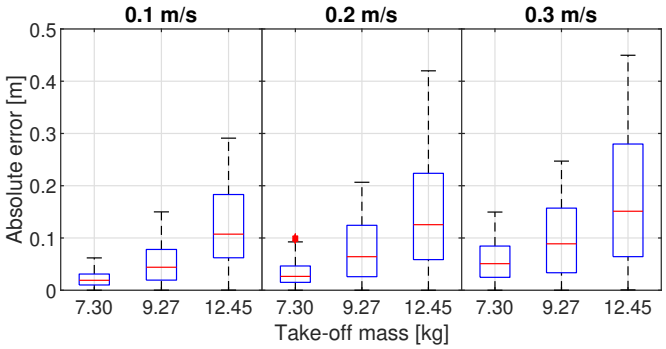

Fig. 6: Box-and-whisker plots to show absolute errors in the x direction while tracking a $0.6\,\mathrm{m}$ radius circular trajectory at $1.8\,\mathrm{m}$ altitude in the motion tracking arena at 3 different speeds.

While carrying high payloads, the ability of the platform to compensate for environmental disturbances was reduced due to the lower TWR. Figure 6 shows that the mean absolute error while tracking a circular trajectory increases strongly with platform mass. Additionally, in an enclosed indoor environment, the platform's own propeller downwash circulates around the room and perturbs the drone in flight. As the hover thrust increases proportionally to the payload, these propwash disturbances become considerably more severe. In an outdoor setting, it is predicted that the trajectory tracking accuracy will improve due to the reduced impact of this effect.

It is envisioned that the platform will be used to demonstrate a number of future aerial construction applications and the requirement may arise for higher payloads and flight times. The current system is reaching the practical size and weight limit for indoor operation, however, a larger system may be desirable for exclusive outdoor operation. There is a capacity for considerably larger motors and batteries without significant modification to the existing frame while maintaining the same propeller size. For example, upgrading to T-motor MN605-S KV170 motors with the same $22\,\mathrm{inch}$ propellers would approximately double the available thrust. Figure 7 shows estimated flight performance curves for such a system with the battery capacity doubled to maintain similar flight times. Including a $75\,\%$ performance reduction due to coaxial rotor interactions and the additional weight of the new components, a maximum payload of $12\,\mathrm{kg}$ is predicted to be feasible.

As the intent is to operate in both indoor and outdoor environments while incorporating the ability to manipulate various tools and interact with surfaces, a control and motion strategy which relies only upon on-board sensing and exhibits the ability to robustly interact with the built and natural environment is required. With these metrics in mind, the use of vision-based state estimation and depth-based object detection is proposed, the framework of which can be seen in Figure 8. Such a sensor suite enables an admittance-based control scheme, ideal for an interactive platform due to its relative simplicity and modularity when implemented within the cascaded

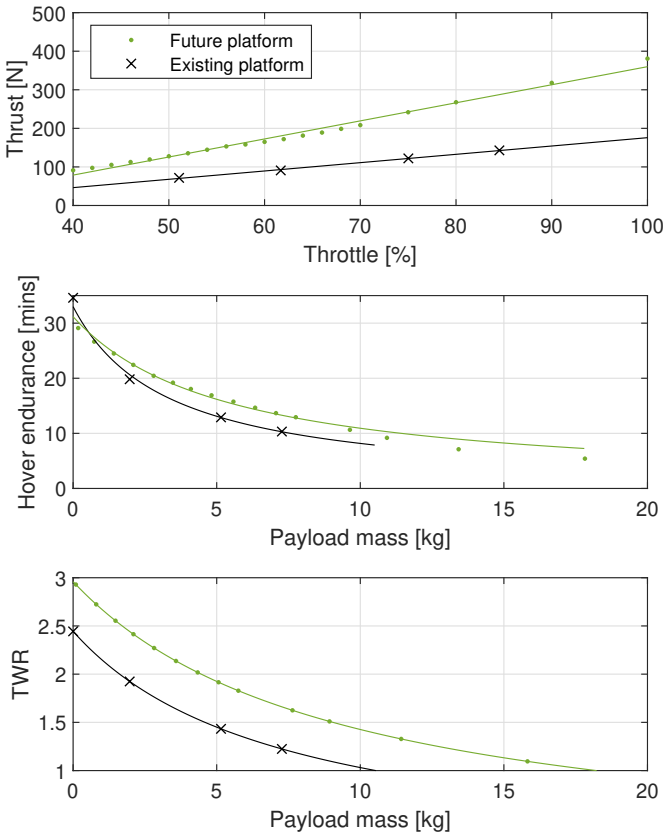

Fig. 7: Estimated performance of an improved platform with larger motors and double battery capacity.

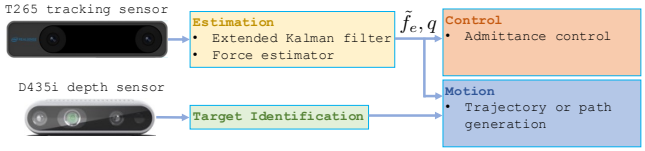

Fig. 8: A visual based tracking sensor, such as the Intel RealSense T265 outputs a state estimate q. An estimate of an external force, $\tilde{f}_e$, facilitates the motion and control of the aerial platform. A depth sensor, shown above as the Intel RealSense D435i, identifies targets and allows motion to be generated to the desired location(s).

control architecture depicted in Figure 9. A salient feature of the proposed control strategy is its ability to integrate with the lower-level PX4 attitude flight controller, with PID parameters carried over from the flight tests described in Section IV. The specific motion generation strategy will vary depending upon the application and environment in which the aerial platform operates.

VI. Conclusions

A high payload platform to meet future challenges in aerial repair and manufacture of infrastructure has been developed. The platform has been tested following trajectories with motion tracking and has been manually flown. The flight testing has confirmed that the platform can meet the desired performance specifications (being able to carry a payload of 5 kg for 13 mins) with a favourable TWR of 1.45. The

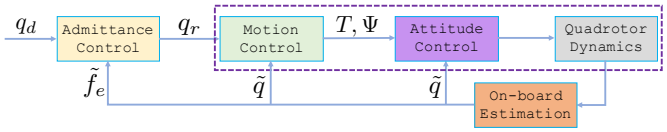

Fig. 9: A proposed control architecture for the aerial platform: an admittance-based controller interfaces with a cascaded motion control architecture contained within the dotted box. In this application, on-board estimation is performed by an IMU, tracking camera and depth camera. Desired and reference states, q_d and q_r, respectively, are defined based on a chosen compliance to an estimated external force, $\tilde{f}_e$, with robot state estimates, $\tilde{q}$, fed back to the control blocks. Admittance and motion control commands are generated on-board the Jetson TX2 compute module, outputting a thrust, T, and attitude, Ψ, command to the Pixhawk 4 flight controller.

platform has been proven to fly stably indoors with payloads up to 7.3 kg. Future work on the platform development will include experimental optimisation of rotor spacing for each coaxial rotor pair and a solution will be developed to reduce mechanical vibration transmission to the flight controller. The design of a manipulator for the platform to perform various construction tasks is underway. It is envisioned that sensors will be integrated to enable a demonstration of full closed-loop manufacturing with visual feedback and it is hoped that work with this platform will direct future large scale aerial robotics research and facilitate novel applications that would be unfeasible at smaller scales.

Acknowledgment

This work was supported by funding from EPSRC (award no. EP/N018494/1, EP/R026173/1, EP/R009953/1, EP/S031464/1, EP/W001136/1), NERC (award no. NE/R012229/1) and the EU H2020 AeroTwin project (grant ID 810321). Mirko Kovac is supported by the Royal Society Wolfson fellowship (RSWF/R1/18003).

References

[1] K. H. Petersen, N. Napp, R. Stuart-Smith, D. Rus, and M. Kovac, "A review of collective robotic construction," *Science Robotics*, vol. 4, no. 28, 2019. [Online]. Available: https://robotics.sciencemag.org/content/4/28/eaau8479

[2] R. Mascaro, M. Wermelinger, M. Hutter, and M. Chli, "Towards automating construction tasks: Large-scale object mapping, segmentation, and manipulation," *Journal of Field Robotics*, vol. n/a, no. n/a. [Online]. Available: https://onlinelibrary.wiley.com/doi/abs/10.1002/rob.22007

[3] "Workplace fatal injuries in great britain," National Statistics, Tech. Rep. July, 2020.

[4] K. Bodie, M. Brunner, M. Pantic, S. Walser, P. Pfändler, U. Angst, R. Siegwart, and J. Nieto, "An Omnidirectional Aerial Manipulation Platform for Contact-Based Inspection," may 2019. [Online]. Available: http://arxiv.org/abs/1905.03502http://dx.doi.org/10.15607/RSS.2019.XV.019

[5] H. Lee, H. Kim, and H. J. Kim, "Planning and control for collision-free cooperative aerial transportation," *IEEE Transactions on Automation Science and Engineering*, vol. 15, no. 1, pp. 189–201, 2018.

[6] A. Farinha, R. Zufferey, P. Zheng, S. F. Armanini, and M. Kovac, "Unmanned aerial sensor placement for cluttered environments," *IEEE Robotics and Automation Letters*, vol. 5, no. 4, pp. 6623–6630, 2020.

[7] P. Chermprayong, K. Zhang, F. Xiao, and M. Kovac, "An Integrated Delta Manipulator for Aerial Repair: A New Aerial Robotic System," *IEEE Robotics & Automation Magazine*, vol. 26, no. 1, pp. 54–66, mar 2019. [Online]. Available: https://ieeexplore.ieee.org/document/8641488/

[8] A. Ollero, M. Tognon, A. Suarez, D. Lee, and A. Franchi, "Past, present, and future of aerial robotic manipulators," *IEEE Transactions on Robotics*, pp. 1–20, 2021.

[9] D. Falanga, K. Kleber, S. Mintchev, D. Floreano, and D. Scaramuzza, "The foldable drone: A morphing quadrotor that can squeeze and fly," *IEEE Robotics and Automation Letters*, vol. 4, no. 2, pp. 209–216, 2018.

[10] P. Zheng, X. Tan, B. B. Kocer, E. Yang, and M. Kovac, "Tiltdrone: A fully-actuated tilting quadrotor platform," *IEEE Robotics and Automation Letters*, vol. 5, no. 4, pp. 6845–6852, 2020.

[11] K. Zhang, P. Chermprayong, D. Tzoumanikas, W. Li, M. Grimm, M. Smentoch, S. Leutenegger, and M. Kovac, "Bioinspired design of a landing system with soft shock absorbers for autonomous aerial robots," *Journal of Field Robotics*, vol. 36, no. 1, pp. 230–251, 2019.

[12] J. Fishman, S. Ubellacker, N. Hughes, and L. Carlone, "Dynamic grasping with a" soft" drone: From theory to practice," *arXiv preprint arXiv:2103.06465*, 2021.

[13] F. Xiao, P. Zheng, J. d. Tria, B. B. Kocer, and M. Kovac, "Optic flow-based reactive collision prevention for mavs using the fictitious obstacle hypothesis," *IEEE Robotics and Automation Letters*, vol. 6, no. 2, pp. 3144–3151, 2021.

[14] B. B. Kocer, M. A. Hady, H. Kandath, M. Pratama, and M. Kovac, "Deep neuromorphic controller with dynamic topology for aerial robots," in *2021 IEEE International Conference on Robotics and Automation (ICRA)*. IEEE, 2021, pp. –.

[15] D. Tish, N. King, and N. Cote, "Highly accessible platform technologies for vision-guided, closed-loop robotic assembly of unitized enclosure systems," *Construction Robotics*, vol. 4, pp. 19–29, 2020.

[16] D. Floreano and R. J. Wood, "Science, technology and the future of small autonomous drones," pp. 460–466, may 2015. [Online]. Available: https://www.nature.com/articles/nature14542

[17] S. Goessens, C. Mueller, and P. Latteur, "Feasibility study for drone-based masonry construction of real-scale structures," *Automation in Construction*, vol. 94, pp. 458–480, oct 2018. [Online]. Available: https://linkinghub.elsevier.com/retrieve/pii/S0926580518301961

[18] Q. Lindsey, D. Mellinger, and V. Kumar, "Construction with quadrotor teams," *Autonomous Robots*, vol. 33, no. 3, pp. 323–336, 2012. [Online]. Available: https://doi.org/10.1007/s10514-012-9305-0

[19] F. Augugliaro, S. Lupashin, M. Hamer, C. Male, M. Hehn, M. W. Mueller, J. S. Willmann, F. Gramazio, M. Kohler, and R. D'Andrea, "The Flight Assembled Architecture installation: Cooperative construction with flying machines," *IEEE Control Systems*, vol. 34, no. 4, pp. 46–64, aug 2014. [Online]. Available: https://ieeexplore.ieee.org/document/6853477/

[20] G. Hunt, F. Mitzalis, T. Alhinai, P. A. Hooper, and M. Kovac, "3D printing with flying robots," in *2014 IEEE International Conference on Robotics and Automation (ICRA)*. IEEE, may 2014, pp. 4493–4499. [Online]. Available: http://ieeexplore.ieee.org/document/6907515/

[21] A. Ollero, G. Heredia, A. Franchi, G. Antonelli, K. Kondak, A. Sanfeliu, A. Viguria, J. Ramiro Martinez-De Dios, F. Pierri, J. Cortes, A. Santamaria-Navarro, M. A. T. Soto, R. Balachandran, J. Andrade-Cetto, and A. Rodriguez, "The AEROARMS Project: Aerial Robots with Advanced Manipulation Capabilities for Inspection and Maintenance," *IEEE Robotics and Automation Magazine*, vol. 25, no. 4, pp. 12–23, dec 2018.

[22] M. Ramasamy, "Hover Performance Measurements Toward Understanding Aerodynamic Interference in Coaxial, Tandem, and Tilt Rotors," *Journal of the American Helicopter Society*, vol. 60, no. 3, pp. 1–17, 2015.

[23] "Facilities — Research groups — Imperial College London." [Online]. Available: https://www.imperial.ac.uk/aerial-robotics/facilities/

[24] "T-MOTOR Store-Official Store for T-motor drone motor,ESC,Propeller." [Online]. Available: https://store-en.tmotor.com/

[25] "Log Analysis using Flight Review — PX4 User Guide." [Online]. Available: https://docs.px4.io/master/en/log/flight{_}review.html